https://doi.org/10.22226/2410-3535-2022-3-255-260

Surface hardening of an Al-Si-Cu-Ni-Mg aluminum alloy by friction stir processing and T6 heat treatment

G.R. Khalikova[†,1,2], G.R. Zakirova[1,2], A.I. Farkhutdinov[2], E.A. Korznikova[1,2,3], V.G. Trifonov[1,2]

[†]gulnara.r.khalikova@gmail.com

[1]Institute for Metals Superplasticity Problems, RAS, Ufa, 450001, Russia
[2]Ufa State Petroleum Technological University, Ufa, 450062, Russia
[3]Ufa State Aviation Technical University, Ufa, 450008, Russia

Friction stir processing (FSP) and standard hardening T6 heat treatment were applied for local surface hardening of the AK12D aluminum (Al-12.8Si-1.67Cu-1.03Ni-0.84Mg-0.33Mn-0.23Co-0.24Fe) alloy plates obtained by hot-compression at elevated temperature. FSP was carried out by introducing a pin into the bulk of the material, followed by its movement along the surface at a traverse speed of 8 and 16 mm/min, accompanied by rotation of the pin at a speed of 2000 rpm. The effect of FSP parameters and T6 treatment on structure and hardness were investigated. It was established that FSP at 2000 rpm and 8 mm/min speed resulted in the formation of a monolithic and defect-free processing zone. The FSP and T6 treatment led to fragmentation of the primary Si and intermetallic phases and partial dissolution of intermetallic phases in the α-Al solid solution followed by decomposition and the formation of dispersed precipitates. The formation of a quasi-equiaxed fine-grained structure was observed after FSP and T6 heat treatment in the stir zone. The measured Brinell hardness demonstrated an average value of 128 HB after treatment versus 103 HB in the initial state. The work reveals the features of the local surface structure refinement allowing to figure out approaches to the design of constructions with enhanced properties.

Keywords: frictions stir processing, heat treatment, Al-Si alloy, microstructure, mechanical properties.

1. Introduction

Aluminum alloys are one of the most common types of construction materials, to which various hardening methods are actively applied, including deformation [1] or thermal treatments [2], surface modification [3] and their combinations [4]. Surface modification of aluminum alloys allows one to improve chemical, physical and mechanical properties, regardless of the properties of the base material. To date, a wide variety of conventional methods of surface hardening of aluminum alloys is reported and analyzed [3]. Multiple drawbacks of existing methods of surface processing of aluminum alloys, including agglomeration of additive particles and their nonuniform distribution, the formation of unwanted phases and interfacial reactions, complicated processing equipment, low processing efficiency, restrict the application of this promising approach. An alternative approach to surface hardening of aluminum alloys that eliminates such defects is friction stir processing (FSP), which is based on the physical principles of friction stir welding. FSP as a method of surface hardening has been tested on a wide range of aluminum alloy compositions [5,6], including the successfully modification of solid-phase state Al-Si alloy [7,8]. The relevance of the approach is defined by the low mechanical properties of the considered alloys due to the presence of coarse Si phase agglomerations [9,10]. For instance, it is shown in [7] that FSP of the cast Al-12Si alloy leads to a significant microstructural refinement and homogenization of eutectic Si particles. The average microhardness is around 21% higher compared to the average hardness value of the cast alloy. Similar results were reported for as-cast A356 aluminum alloy [8]. FSP resulted in significant fragmentation of coarse acicular Si particles and primary aluminum dendrites, created a uniform distribution of Si particles in the aluminum matrix, and nearly eliminated all casting porosity. These FSP induced microstructural modifications significantly improved the tensile properties at room temperature of cast A356, in particular, ductility. In [8], it is also reported that the ultimate tensile strength and ductility of FSP-ed samples with followed by T6 treatment are significantly higher than those of cast A356. However, both FSP-ed and cast samples exhibited similar yield strengths.

Although FSW/FSP eliminates the problem caused by the presence of a fusion zone, the associated evolution of the microstructure can still be a reason of the degradation of mechanical properties [11,12]. Recovering of the level of mechanical properties after FSW/FSP is a subject of study of particular importance especially considering the fact that the operation of friction stir obtained constructions often takes place at elevated temperatures. Therefore, the stability of the processing zone after FSW/FSP is also of importance. Al-Si alloys belong to the group of materials where the post treatment hardening is achieved by post deformational thermal treatment leading to aging induced precipitation of intermetallic particles, which, in turn increase the contribution of dispersion hardening to the overall strength of the material. Several authors have reported improvements in mechanical

properties after post-weld heat treatment [13,14], whereas others have demonstrated the degradation of mechanical properties after the thermal treatment associating the strength decrease with the abnormal grain growth [11,15,16].

The purpose of this work was to evaluate the possibility of local surface hardening of the AK12D aluminum alloy in the solid state by friction stir processing and T6 heat treatment.

2. Materials and experimental methods

Commercial aluminum alloy AK12D used in this study has the following chemical composition: Al-12.8%Si-1.67%Cu-1.03%Ni-0.84%Mg-0.33%Mn-0.23%Co-0.24%Fe (wt.%). A hot-compressed rod of the AK12D alloy was subjected to hot deformation by 50% at 450°C. The final thickness of the sample after compression was 12 mm. The required degree of surface roughness was achieved by mechanical processing. Single-pass friction stir processing (FSP) was carried out on an upgraded milling machine (see Video_1.mp4 file, supplementary material). A processing tool with a cone-shaped pin was used. The speed modes of the machining tool were: rotational speed ω — 2000 rpm, traverse speed v — 8 and 16 mm/min. FSP treated samples were subjected to standard hardening T6 heat treatment according to the following regime: quenching at a temperature of 520°C and subsequent artificial aging at 190°C for 10 hours.

Microstructure investigations were performed for both the initial alloy (AK12D-T6) and FSP-ed alloy after T6 heat treatment (AK12D-FSP-T6). For macro- and microstructural observations, AK12D-T6 and AK12D-FSP-T6 alloys were etched in the solution: H_2O (60 ml), HNO_3 (35 ml), HF (5 ml). The volume fraction of primary phases and precipitates was obtained from the scanning electron microscopy (SEM) analysis of the polished samples. Details of the macrostructure of the cross-sections of the FSP-ed were analyzed using a Zeiss Axio Scope.A1 optical microscope. Microstructural studies were carried out using a Tescan Mira 3LMH scanning electron microscope with secondary electron (SE) and backscattered electron (BSE) detectors. The modification effects of FSP on the mechanical behavior were investigated using Vickers microhardness and Brinell hardness. Mechanical properties were evaluated in both the AK12D-T6 and AK12D-FSP-T6 alloys. Vickers microhardness was carried out using Axiover-100A microhardness testers under a load of 100 g. Hardness measurements were evaluated in the longitudinal section of the FSP-ed zone of AK12D-FSP-T6 alloys. Rockwell hardness was carried out using a TP 5006 Rockwell hardness testing machine. The resulting HRB hardness values were converted to HB values. The results were processed with a 95% confidence level.

3. Results

3.1. Initial microstructure

Figure 1 shows typical microstructures of the initial (base metal) AK12D aluminum alloys after T6 heat treatment. The AK12D-T6 alloy contains elongated particles of primary and strengthening intermetallic phases, oriented along the direction of material flow in the hot deformation process. According to [17], in Al-Si-Cu-Ni-Mg-Mn-Fe alloys the following primary intermetallic phases can exist: Al_5FeSi, Al_8Fe_2Si, $Al_{15}(Fe,Mn)_2Si$, $FeNiAl_9$, $Al_8FeMg_3Si_6$, Al_3Ni, Al_7Cu_4Ni, $Al_3(Ni,Cu)_2$, Al_2Cu, Mg_2Si, $Al_6Cu_2Mg_8Si_5$. The use of hardening T6 heat treatment can result in the formation of Al_2Cu, Mg_2Si, $Al_5Cu_2Mg_8Si_6$, Al_2CuMg metastable precipitates. A quantitative assessment of the dimentinal characteristics of the phases of the AK12D-T6 alloy is given in Table 1. The grain structure of the alloy in its initial state is recrystallized with an average grain size of 11.5 ± 0.4 μm. The measured values of microhardness and hardness of the initial AK12D-T6 alloy are 143 ± 2 HV and 103 HB, accordingly.

3.2. Macrostructure

In our case, typical macrostructures of the AK12D-FSP-T6 alloy are shown in Fig. 2. At deformation speeds ω = 2000 rpm and v = 8 mm/min, the FSP-ed zone has a basin-shaped stir zone. It is elongated and asymmetrical by relation to

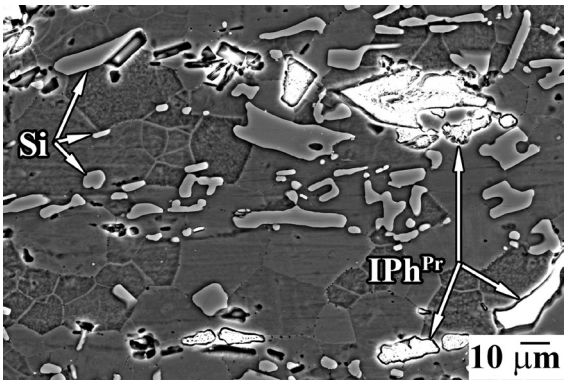

Fig. 1. A typical microstructure of initial AK12D aluminum alloys. Etched sample.

Table 1. Average area (S, μm²) and volume fraction (V, %) of primary phases (Pr) of Si and intermetallic particles (IPh) and precipitates (Sec), average grain size (d) and mechanical properties (HV, HB) of AK12D aluminum alloy after FSP and T6 heat treatment.

Alloy		AK12D-T6		AK12D-FSP-T6					
Zone		Initial/BM		SZ-1		SZ		TMAZ	
		S, μm²	V, %	S, μm²	V, %	S, μm²	V, %	S, μm²	V, %
Si	Pr	45.9 ± 5.7	13 ± 1	13.9 ± 1.1	12 ± 1	7.4 ± 0.5	13 ± 1	32.7 ± 3.6	13 ± 1
IPh	Pr	39.9 ± 4.0	8 ± 1	5.2 ± 1.2	5 ± 1	2.0 ± 0.4	3 ± 1	22.4 ± 6.5	7 ± 1
	Sec	0.026 ± 0.005	1 ± 0.5	0.043 ± 0.004	4 ± 0.5	0.035 ± 0.002	6 ± 0.5	0.035 ± 0.005	1 ± 0.5
d, μm		11.5 ± 0.4		10.3 ± 0.2		3.3 ± 0.1		9.6 ± 0.5	
HV		143 ± 2		147 ± 3		134 ± 2		137 ± 3	
HB		103		128					

the central line of the stir zone. The FSP-ed zone expands dramatically when approaching the workpiece surface. At deformation speeds ω = 2000 rpm and v = 16 mm/min, the FSP-ed zone forms a basin-shaped stir zone with a uniform expansion of its boundaries to the surface of the workpiece, and having a tunnel defect on the advancing side. A stir zone (SZ), a thermomechanically affected zone (TMAZ) and a base metal (BM) zone can be distinguished in the structure of the alloy after complex treatment. No distinct boundary between the heat-affected zone and base metal can be identified. Microstructural study of the FSP-ed sample revealed the complex structure of the stir zone containing a large number of turbulent material flows formed by the movement of the pin along the tool contour (Fig. 2 a). On opposite sides of the stir zone, there are bending areas with different structure types (dark in AS and light areas in RS), alternationg in its central part. This type of structure appears to be similar to the so-called "onion ring" pattern addressed in [18].

3.3. Microsrtucture

Microstructural investigations revealed that primary Si and intermetallic phases are subjected to fragmentation during the FSP process, while partial dissolution is observed only for the intermetallic component (Fig. 3, Table 1). In addition, from the advancing side of the FSP-ed zone, fragmentation

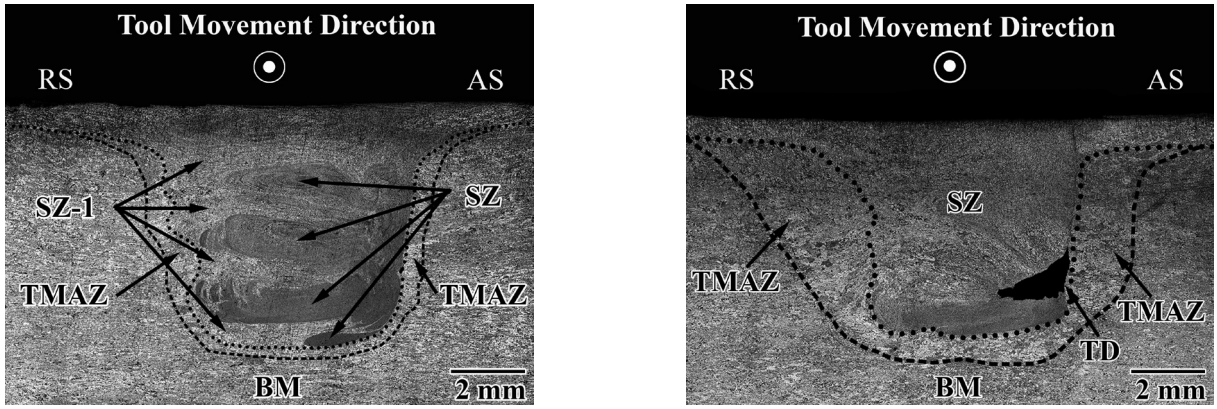

a b

Fig. 2. Optical macrograph showing typical different zones at the FSP-ed region of AK12D alloy at the: ω = 2000 rpm, v = 8 mm/min (a); ω = 2000 rpm, v = 16 mm/min (b). RS — retreating side; AS — advancing side; SZ — stir zone; TMAZ — thermomechanically affected zone; BM — base metal; TD — tunnel defect. Etched samples.

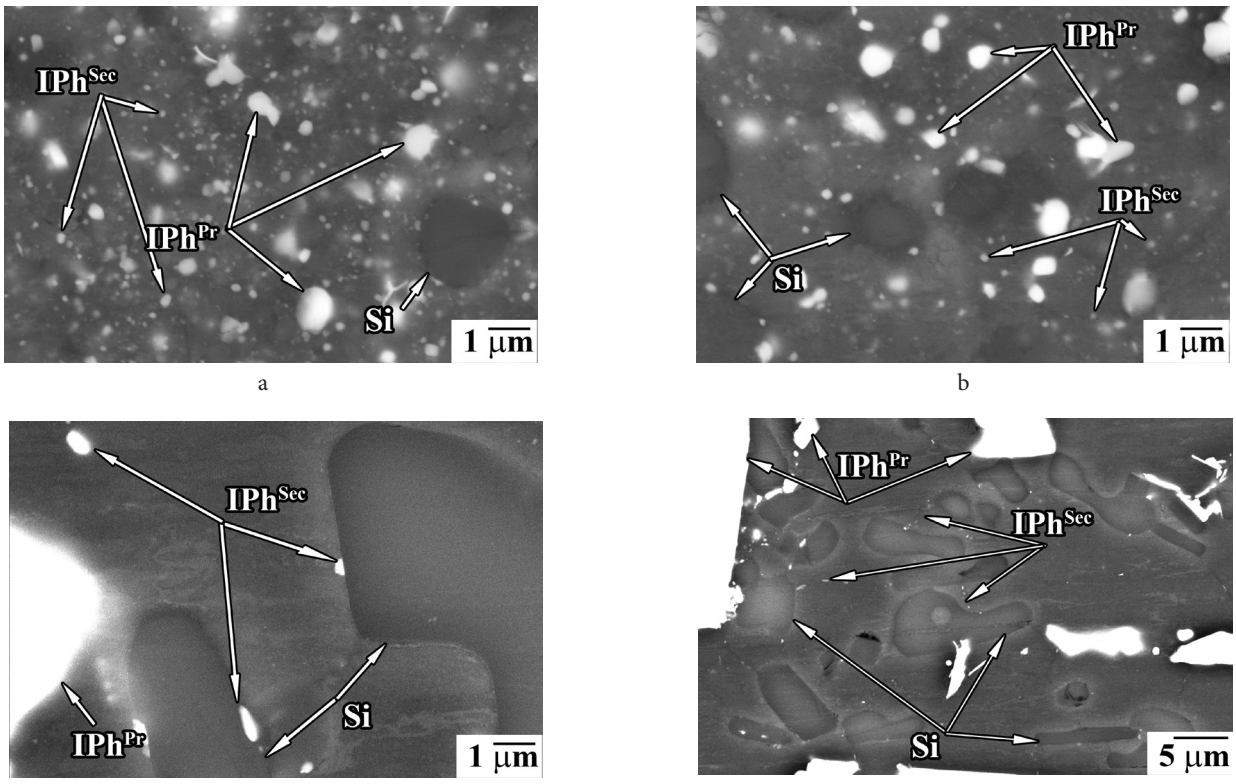

a b

c d

Fig. 3. Typical microstructures of the AK12D alloy after friction stir processing at ω = 2000 rpm and v = 16 mm/min and subsequent T6 heat treatment: stir zone-1 (a), stir zone (b), thermomechanically affected zone (c), base metal (initial state) (d). Polished samples. White particles are intermetallic phases, gray particles are silicon (BSE imaging mode).

and dissolution occurs faster (dark areas SZ in Fig. 2), than from the retreating side (light areas SZ-1 in Fig. 2). The corresponding microstructures of the SZ and SZ-1 regions at high magnifications are shown in Figs. 3 a and b, respectively. The formation of supersaturated α-Al in the stir zone during FSP leads to its decay in the heat treatment. In SZ, the average area of the dispersed precipitates is smaller compared to SZ-1, and the volume fraction of the precipitates in SZ is larger compared to SZ-1 (Table 1). This is due to the different degree of alloying of the α-Al solid solution in these areas during the FSP process, which, in turn, is caused by the difference in the temperatures of the material in the retreating and advancing sides. Fragmented particles of primary phases are observed in TMAZ. Their average size is smaller compared to the initial state, while maintaining a constant volume fraction (Table 1). In the TMAZ of the AK12D-FSP-T6 alloy precipitates (Fig. 3 c) with an average size and volume fraction comparable to those in the AK12D-T6 alloy (Fig. 3 d, Table 1) are detected.

An analysis of the grain structure revealed the formation of a quasi-equiaxed fine-grained structure in the stir zone (Fig. 4) after complex treatment. On the advancing side, the average grain size in the stir zone is smaller than that on the retreating one. In TMAZ, a slight stretching of the initial grains in the direction of the material flow and a slight decrease in their average size are observed. The average grain sizes in different zones of the sample subjected to FSP and T6 treatment are given in Table 1.

3.4. Mechanical properties

The results of microhardness measurement are given in Table 1. It can be seen that in the AK12-FSP-T6 alloy, the microhardness in the SZ is lower than that in SZ-1. At the same time, in TMAZ, the microhardness does not change compared to the base metal (initial AK12D-T6 alloy). The results of the Brinell hardness measurements for the AK12D-FSP-T6 alloy showed that the hardness values increased from 103 to 128 HB for the AK12D-T6 alloy.

4. Discussion

Depending on the processing parameters, tool geometry, temperature of the workpiece, and thermal conductivity of the material, various shapes of the stir zone can be observed [19]. The formation of basin-shaped stir zones observed in the study (Fig. 2 a) during friction stir processing is highly likely the result of extreme deformation experienced by the upper surface and frictional heating due to contact with a cylindrical-tool shoulder during FSP [20]. However, depending on the processing parameters, various defect types can be formed [21–23]. Treatment at a traverse speed of 16 mm/min leads to the initiation of a tunnel defect on the advancing side (Fig. 2 b) due to smaller deformations of the plasticized material caused by insignificant heat release, and, as a result, a lower peak temperature of the material in the mixing zone [24]. It can be noted that a flow of the material from the retreading side (RS) to the advancing side (AS) takes place during FSP. Lower temperatures on RS mean that there is insufficient straining on AS and hence, defects appear on AS, as one can see in Fig. 2 b. Higher temperature at the tool shoulder suggests that the shoulder is able to strain the material on AS. However, since the temperatures at the tool pin are much lower, there is much less plastic flow, hence, a void is left behind. On the chance of a traverse speed of 8 mm/min, the flow rate of the material allows the resulting void to be filled and forms a monolithic and defect-free machining area (Fig. 2 a), which is not the case for the traverse speed of 16 mm/min (Fig. 2 b).

The authors of [25] also observed the earlier mentioned formation of complex flows of the alloy along the contour of the tool motion accompanied by the generation of a complexly organized multi-nugget stir zone with small separate vortex zones.

FSP can be considered as a local hot-working process where microstructural changes in the treatment area are caused by thermomechanical effects due to friction between the tool and the workpiece and plastic deformation around the rotating pin. FSP creates a softened region around the center of the processing area in the AK12D aluminum alloy. The temperature gradient initiated by the non-homogenous distribution of the frictional heat results in the corresponding difference of primary phases fragmentation and partial dissolution of intermetallic phases and produced a range of precipitates from the center of the SZ to the BM. Post FSP solution heat treatment can lead to the decomposition of the supersaturated solid solution and the formation of dispersed precipitations. Depending on the thermomechanical effects during FSP, affecting the dissolution of the primary

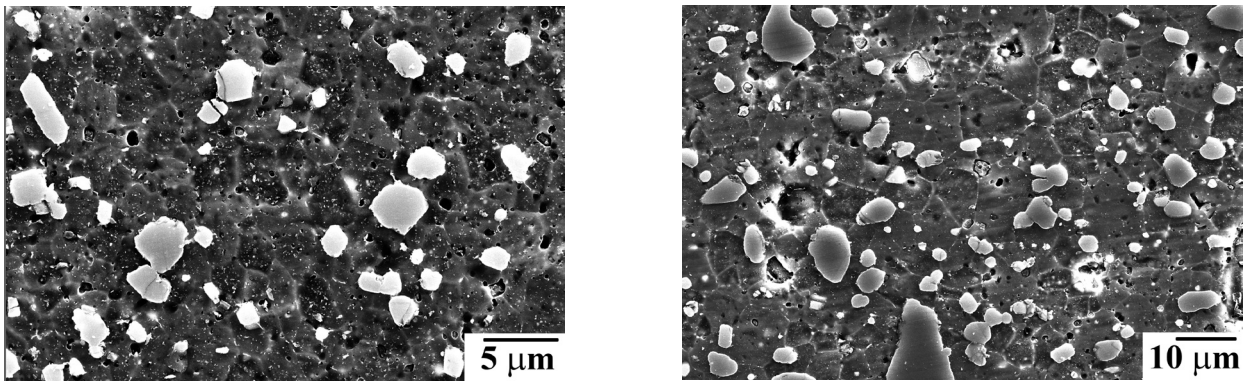

a b

Fig. 4. Typical grain microstructures of the AK12D alloy after friction stir processing at ω = 2000 rpm and *v* = 16 mm/min and subsequent T6 heat treatment: stir zone (a), stir zone-1 (b) (SE imaging mode). Etched samples.

intermetallic phases, the average surface and volume fraction of precipitations changes accordingly after the solution heat treatment.

It is widely known [26, 27] that the post FSW/FSP high temperature treatment can make a totally different impact on the grain structure stability. In AK12D-FSP-T6, a fine-grained structure was preserved. This can be explained by the presence of a large amount of fragmented excess phases in the alloy structure stabilizing the growth of recrystallized grains during subsequent solution heat treatment. Similar results are given, for example, in [27].

The observed structural changes do not significantly affect the changes in microhardness in the treatment zone compared to the base metal after hardening heat treatment (Table 1). In general, changes in microhardness in different zones of the processing area and the base metal after heat treatment do not exceed 6%. The investigated alloy has a complex chemical composition with a large number of coarse primary phases, and the measurement of microhardness at local points did not provide, in this case, any important information. Therefore, one could consider the change in Brinell hardness as a more integral value, taking into account the heterogeneity of the microstructure. It was revealed that the hardness of the AK12D alloy after FSP and T6 heat treatment increases from 103 to 128 HB. This is due to the refinement of the primary phases and dispersed precipitates formation. A similar increase in hardness is shown for a number of aluminum alloys, the grain structure of which did not undergo abnormal growth during post deformational heat treatment [28].

5. Conclusions

As a result of this work, the FSP mode and hardening T6 heat treatment were developed, allowing one to achieve the formation of a monolithic defect-free structure in the AK12D (Al-12.8Si-1.67Cu-1.03Ni-0.84Mg-0.33Mn-0.23Co-0.24Fe) alloy with a high level of mechanical properties. The FSP mode at a rotation speed of 2000 rpm and a traverse speed of 8 mm/min resulted in the formation of a monolithic and defect-free treatment zone. The complex treatment led to the formation of an inhomogeneous microstructure in the FSP-ed area with different zones. In the stir zone, intensive fragmentation of primary phases and partial dissolution of primary intermetallic particles of in the α-Al solid solution followed by its decomposition and the formation of dispersed precipitates was demonstrated. A fine-grained structure, with an average grain size of 3.3 ± 0.1 and 10.3 ± 0.2 μm, was formed in the stir zone. Brinnel heardness increased from 103 HB for initial state and T6 heat treatment alloy to 128 HB for the structure after friction stir processing and T6 heat treatment alloy. The results obtained in the work contribute to the development of technological methods for local hardening of industrial aluminum alloys due to the formation of a dispersed microstructure with a high level of mechanical properties.

Supplementary material. *The online version of this paper contains supplementary material available free of charge at the journal's Web site (lettersonmaterials.com).*

Acknowledgements. Friction stir processing modes, macrostructural studies and hardness measurements were carried out at the expense of the Russian Science Foundation grant No. 22-29-01318. Microstructural studies on a scanning electron microscope and microhardness measurements were carried out on the facilities of shared services center of the Institute for Metals Superplasticity Problems of Russian Academy of Sciences "Structural and Physical-Mechanical Studies of Materials" and the studies were supported by the Ministry of Science and Higher Education of the Russian Federation under the state assignment of IMSP RAS. E. A. Korznikova is grateful for financial support to the Ministry of Science and Higher Education of the Russian Federation within the framework of the state task of the USATU (No. 075-03-2022-318/1) of the youth research laboratory "Metals and Alloys under Extreme Impacts".

References

1. G. R. Khalikova, G. F. Korznikova, V. G. Trifonov. Lett. Mater. 7 (1), 3 (2017). (in Russian) Crossref
2. M. Myshlyaev, S. Mironov, G. Korznikova, T. Konkova, E. Korznikova, A. Aletdinov, G. Khalikova, G. Raab, S. L. Semiatin. J. Alloys Compd. 898, 162949 (2022). Crossref
3. I. Hutchings, Ph. Shipway. Tribology: friction and wear of engineering materials. Second Edition. Oxford, United Kingdom, Butterworth-Heinemann (2017) 237 p.
4. R. R. Mulyukov, G. F. Korznikova, K. S. Nazarov, R. K. Khisamov, S. N. Sergeev, R. U. Shayachmetov, G. R. Khalikova, E. A. Korznikova. Acta Mech. 232, 1815 (2021). Crossref
5. A. Heidarzadeh, S. Mironov, R. Kaibyshev, G. Çam, A. Simar, A. Gerlich, F. Khodabakhshi, A. Mostafaei, D. P. Field, J. D. Robson, A. Deschamps, P. Withers. J. Prog. Mater. Sci. 117, 100752 (2021). Crossref
6. A. P. Zykova, S. Yu. Tarasov, A. V. Chumaevskiy, E. A. Kolubaev. Metals. 10 (6), 772 (2020). Crossref
7. H. Sun, S. Yang, D. Jin. Trans. Indian Inst. Met. 71, 985 (2018). Crossref
8. Z. Y. Ma, S. R. Sharma, R. S. Mishra. Metall. Mater. Trans. A. 37, 3323 (2006). Crossref
9. P. Ma, Y. D. Jia, K. G. Prashanth, Z. S. Yu, C. G. Li, J. Zhao, S. L. Yang, L. X. Huang. J. Mater. Res. 32 (11), 2210 (2017). Crossref
10. J. Abboud, J. Mazumder. Sci. Rep. 10, 12090 (2020). Crossref
11. M. W. Mahoney, C. G. Rhodes, J. G. Flintoff, R. A. Spurling, W. H. Bingel. Metall. Mater. Trans. A. 29, 1955 (1998). Crossref
12. W. D. Lockwood, B. Tomaz, A. P. Reynolds. Mater. Sci. Eng. A. 323, 348 (2002). Crossref
13. M. Cabibbo, H. J. McQueen, E. Evangelista, S. Spigarelli, M. Di Paola, A. Falchero. Mater. Sci. Eng. A. 460 – 461, 86 (2007). Crossref
14. K. Elangovan, V. Balasubramanian. Mater. Charact. 59, 1168 (2008). Crossref
15. K. V. Jata, K. K. Sankaran, J. J. Ruschau. Metall. Mater. Trans. A. 31, 2181 (2000). Crossref

16. A. Sullivan, J.D. Robson. Mater. Sci. Eng. A. 478, 351 (2008). Crossref
17. N.A. Belov. Phase composition of industrial and advanced aluminum alloys: monograph. Moscow, MISIS (2010) 511p.
18. G.R. Cui, Z.Y. Ma, S.X. Li. Scripta Mater. 58, 1082 (2008). Crossref
19. R.S. Mishra, Z.Y. Ma. Mater. Sci. Eng. R. 50, 1 (2005). Crossref
20. Y.S. Sato, H. Kokawa, M. Enomoto, Sh. Jogan. Metall. Mater. Trans. A. 30, 2429 (1999). Crossref
21. N. Murugan, B. Ashok Kumar. Mater. Des. 51, 998 (2013). Crossref
22. N. Sharma, Z.A. Khan, A.N. Siddiquee. Trans. Nonferrous Met. Soc. China. 27, 2113 (2017). Crossref
23. Q. Qin, H. Zhao, J. Li, Y. Zhang, X.Su. Trans. Nonferrous Met. Soc. China. 30, 2355 (2020). Crossref
24. T. Hirata, T. Oguri, H. Hagino, T. Tanaka, S.W. Chung, Y. Takigawa, K. Higashi. Mater. Sci. Eng. A. 456 (1–2), 344 (2007). Crossref
25. T. Kalashnikova, A. Chumaevskii, K. Kalashnikov, S. Fortuna, E. Kolubaev, S. Tarasov. Metals. 10, 806 (2020). Crossref
26. X.-G. Chen, M. da Silva, P. Gougeon, L. St-Georges. Mater. Sci. Eng. A. 518 (1-2), 174 (2009). Crossref
27. W. Gan, K. Okamoto, S. Hirano, K. Chung, C. Kim, R.H. Wagoner. J. Eng. Mater. Technol. 130 (3), 031007 (2008). Crossref
28. P. Maji, R.K. Nath, R. Karmakar, P. Paul, R.K. Bhogendro Meitei, S.K. Ghosh. CIRP J. Manuf. Sci. Technol. 35, 96 (2021). Crossref